Development of a hybrid mode linear transformer driver stage

Le Zhang,[*] Meng Wang, Liangji Zhou, Qing Tian, Fan Guo, Lingyun Wang, Yanling Qing,
Yue Zhao, Yingmin Dai, Wenhui Han, Lin Chen, and Weiping Xie

Key Laboratory of Pulsed Power, Institute of Fluid Physics, China Academy of Engineering Physics,
P.O. Box 919-108, Mianyang 621900, China

At present, the mainstream technologies of primary power sources of large pulse power devices adopt Marx or linear transformer driver (LTD) designs. Based on the analysis of the characteristics of these two types of circuit topologies, the concept of a hybrid mode LTD stage based on Marx branches is proposed. The analysis shows that the hybrid mode LTD stage can realize the following goals: (a) to reduce the energy and power handled by the basic components (switch and capacitor) to lengthen their lifetime; (b) to reduce the requirements of the multipath synchronous trigger system; and (c) to improve the maintainability of the LTD stage by using independent Marx generators instead of "traditional LTD bricks." To verify the technique, a hybrid mode LTD stage consisting of 50 branches (four-stage compact Marx generators) was designed, manufactured and tested. The stage has a radius of about 3.3 m and a height of 0.6 m. The single Marx circuit's load current is about 21 kA, with a rise time of ~90 ns (10%–90%), under the conditions of capacitors charged to ±40 kV and a 6.9 Ω matched load. The whole stage's load current is ~1 MA, with a rise time of ~112 ns (10%–90%), when the capacitors are charged to ±45 kV and the matched load is 0.14 Ω.

I. INTRODUCTION

Commercial application of controlled thermonuclear fusion energy is an ideal approach to solve human energy needs for the future. A fusion-fission hybrid reactor technology based on the Z-pinch technique is one possible way to achieve this goal [1–4]. As the fundamental and core technology, a high-power repetitive Z-pinch driver requires significant research progress in a relatively short period of time, to provide the necessary experimental platform for fusion target, driver or hybrid reactor development. In recent years, many high-power repetitive driver designs based on linear transformer drivers (LTDs) have been proposed [5–8].

According to preliminary conceptual designs, for the commercial application, the Z-pinch driver should have a lifetime of more than 10^6 shots. However, the lifetime of basic components and the synchronization of the large number of switches are inevitable technical problems. As a solution, we put forward the concept of a hybrid mode LTD stage based on Marx branches [9].

Through circuit topology analysis, we verify that the output parameters of a hybrid mode LTD stage including Marx circuits are in complete accord with series LTD stages with the same components. Based on this, the design of a hybrid mode LTD stage based on four-stage coaxial Marxes is presented. The hybrid mode LTD stage contains 50 independent coaxial Marxes, and the output end of the Marxes are connected to the periphery of a magnetic core inductive cavity via transmission lines. The Marxes can be adjusted and installed independently, effectively reducing the engineering difficulty of the stage and improving the maintainability of the stage. Based on this preliminary analysis, the development of two key components, the long-life gas spark-gap switch and the capacitor, was carried out. Both the switch and capacitor were tested more than 170 000 times under the condition of ±40 kV/20 kA/0.1 Hz. Next, we developed a four-stage coaxial Marx, whose two front switches are triggered and two last switches are self-triggered from overvoltage breakdown. For this step, the Marx's required time jitter is satisfied and the performance requirement and complexity of the trigger system is effectively reduced (compared with the equivalent LTD). The experimental results show that, under the condition of ±40 kV/20 kA/0.1 Hz, the Marx can operate continuously more than 20,000 times. After the development of auxiliary systems such as a charge system, trigger system, control system and reset system, the development of a hybrid mode LTD stage was completed. The whole stage's load current is ~1 MA, with a rise time of ~112 ns (10%–90%), with the capacitors charged to ±45 kV and the matched load is 0.14 Ω.

---
[*]Corresponding author.
6157681@qq.com

II. ANALYSIS OF HYBRID MODE LTD CIRCUIT TOPOLOGY

The Marx generator is a mature technology with the longest application time in pulse power systems. Both Marx and LTD circuits are based on capacitive energy storage and closing switches, whereby the Marx [10–12] adopts pure series topology and the LTD [13] adopts pure parallel topology. The difference between the two topologies results in a great difference in their working characteristics.

As shown in Fig. 1, when the basic components number and parameters are fixed, parallel branches (n) multiplied by series stages (m) is constant (k = mn), so m and n are inversely related. With a matched load, the output current I is inversely proportional to the output voltage V, i.e., the total output power is constant. It can be seen that the Marx generator and the LTD stage work in two extreme modes respectively, namely the Marx circuit (n = 1, m = k) and the LTD circuit (n = k, m = 1).

We consider the case of equal components number and parameters: 2n capacitors (capacitance C_0, charging voltage $\pm V_0$), n switches, and assume that the corresponding two capacitors and one switch are in a low-inductance connection (inductance L_0). This paper's analysis ignores the influence of circuit resistance. Whether Marx or LTD, the circuit consists of capacitive energy storage and a closing switch. Therefore, they can both be modeled by the same simplified circuit (ignoring circuit resistance and magnetic core loss), shown in Fig. 2.

For the Marx, all components are in series and one Marx consists of n basic discharge stages. In the case of maximum load output power, the output pulse rise time, matched impedance and output voltage are, respectively,
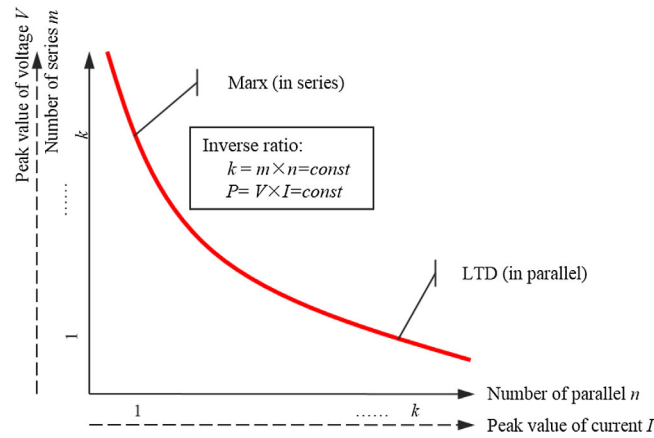

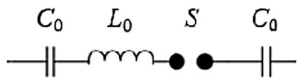FIG. 1. Inverse relationship of different circuit topologies.

FIG. 2. Simplified basic discharge circuit.

$$\tau_{\text{Marx}} \propto \sqrt{LC} = \sqrt{(nL_0)\left(\frac{C_0}{2n}\right)} = \frac{1}{\sqrt{2}}\sqrt{L_0 C_0}$$

$$Z_{\text{Marx}} \propto \sqrt{L/C} = \sqrt{(nL_0)/\left(\frac{C_0}{2n}\right)} = \sqrt{2}n\sqrt{L_0/C_0}$$

$$V_{\text{out,Marx}} \approx nV_0.$$

For the LTD, two capacitors and one switch form one basic discharge circuit, and then n such circuits are connected in parallel to form one stage. Likewise, in the case of maximum load output power, the output pulse rise time, matched impedance and output voltage are, respectively,

$$\tau_{\text{LTD}} \propto \sqrt{LC} = \sqrt{\left(\frac{L_0}{n}\right)\left(\frac{C_0}{2}n\right)} = \frac{1}{\sqrt{2}}\sqrt{L_0 C_0}$$

$$Z_{\text{LTD}} \propto \sqrt{L/C} = \sqrt{\left(\frac{L_0}{n}\right)/\left(\frac{C_0}{2}n\right)} = \frac{\sqrt{2}}{n}\sqrt{L_0/C_0}$$

$$V_{\text{out,LTD}} \approx V_0.$$

It can be seen that: (i) in the case of equal components number and parameters, the output pulse rise time of the pure series Marx circuit and the pure parallel LTD circuit are the same. (ii) The matched impedance of the Marx circuit is n^2 times that of the LTD circuit, and the corresponding output voltage is n times greater. In the same energy storage situation, the electrical power obtained on the load ($P = V^2/Z$) is equal, and the LTD output current is n times that of the Marx. It can be inferred that the LTD stage circuit topology can greatly reduce the output matched impedance, and increase the stage's output current, which are advantages for the design of large, low impedance pulse power devices.

On the basis of the previous analysis, the possibility of introducing the Marx circuit into multiple LTD series stages is proposed. As shown in Fig. 3, there is a series of m LTD stages (defined as a series module), each stage consists of n bricks, and each brick consists of two capacitors and one switch, therefore there are 2 m × n capacitors and m × n switches.

The bricks of the m LTD stages in the dashed frame are combined to form one independent Marx branch, so that the n Marx branches are connected in parallel, namely, one hybrid mode LTD stage. The results of Table I can be derived by using the same component and parameter assumptions above.

As can be seen from Table I, after the introduction of the Marx branch, the output parameters of the hybrid mode LTD stage are exactly the same as the traditional series LTD stages. Within a certain range of m values, the circuit topology of this hybrid mode LTD stage is between pure series and pure parallel. This design can take advantages of the beneficial features of both circuits and avoid some technical difficulties to a certain extent.
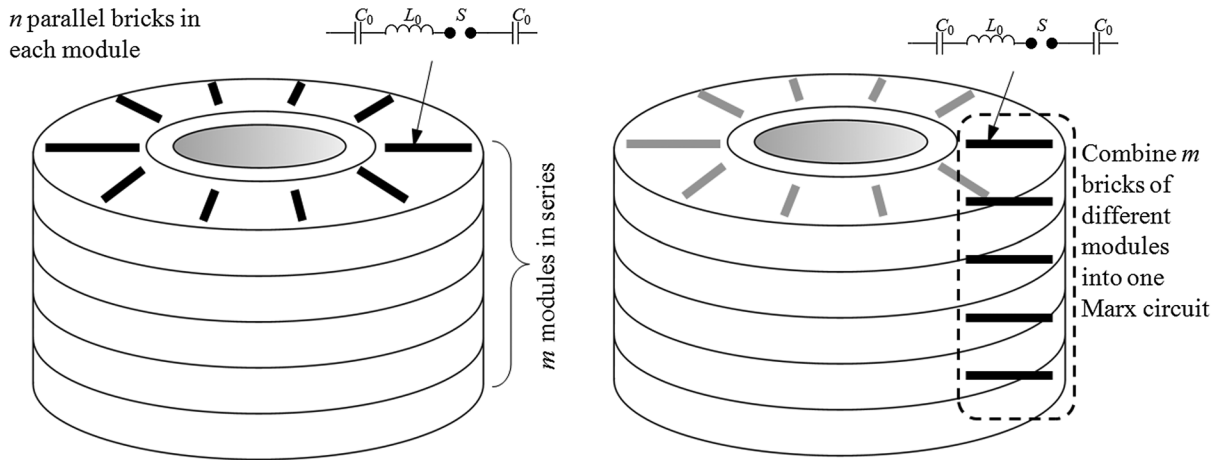
FIG. 3.   Construction of hybrid mode LTD stage.

III. DESIGN OF HYBRID MODE LTD STAGE

One advantage of the Marx is that only the first few switches need to be triggered, and the latter-stage switches work in the overvoltage self-breakdown mode, which can reduce the requirement of the LTD trigger system, where all switches must be triggered. Therefore, if m is too small, the overvoltage coefficient of the latter-stage switches is limited, which can lead to increased jitter of the switch closure and affect the rise time of the output pulse. On the other hand, the output voltage of the Marx is proportional to m. So, if m is too large, the output voltage of a single branch is too high, which can make the insulation design of the stage more difficult.

We chose the value of m as 4, considering our purpose is just to verify the concept of hybrid mode LTD and not to solve a complex engineering problem. At this point, if only the first two switches are triggered, the requirement for the trigger system is reduced by about one half. If the charge voltage of the capacitor is reduced from about 90 kV to about 40 kV, the maximum output voltage of the single Marx branch is about 300 kV, which is an acceptable value for insulation requirements. Meanwhile, the capacitor and switch lifetimes at the lower voltage level would be greatly increased. The independent Marx branch is much easier to disassemble, so the whole stage is easier to maintain. In addition, the project scale of a hybrid mode LTD stage is modest. Therefore, the proposed hybrid mode LTD technology can meet the requirements of a z-pinch fusion energy driver with repetitive operation (∼0.1 Hz), long lifetime (>10^6 times) and improved maintainability [14].

Based on the above design, and taking the development experience of a 1 MA single LTD stage platform and a 1 MV series LTD platform of our institute as references [15], the design scheme of the hybrid mode LTD stage is proposed as follows: (i) Each single Marx discharge branch has an open circuit voltage of about 300 kV, and the output voltage is about 150 kV on matched load. (ii) Each discharge branch has a four-stage Marx structure (m = 4, i.e., four switches, eight capacitors), the first two switches are triggered, and the last two switches work in the overvoltage self-breakdown mode. (iii) A single stage consists of 50 parallel branches, and each branch current (that is, switch current) is about 20 kA, to optimize the lifetime potential of the components. (iv) Two layers (25 branches per layer) are used in parallel to reduce the diameter of the stage.

The design of the hybrid mode LTD stage based on the Marx circuit is shown in Fig. 4. The hybrid mode LTD stage consists of 50 independent coaxial Marx branches, corresponding transmission lines and converging cavity. The stage has a radius of about 3.3 m and a height of 0.6 m. The relevant electrical parameters of each part are shown in Table II.

TABLE I.   Parameter comparisons of the hybrid mode LTD stage and series LTD stages.

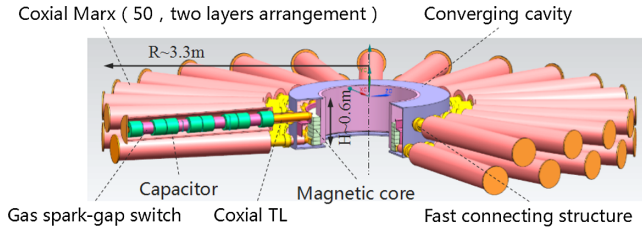| Parameter	Series LTD stages		Hybrid mode LTD stage	
	Single LTD	m series LTD stages	Single marx	n Marx in parallel
Current rise time	$\sqrt{2}\cdot\sqrt{L_0 C_0}$	$\sqrt{2}\cdot\sqrt{L_0 C_0}$	$\sqrt{2}\cdot\sqrt{L_0 C_0}$	$\sqrt{2}\cdot\sqrt{L_0 C_0}$
Matched impedance	$1.1\sqrt{2}\cdot\frac{1}{n}\cdot\sqrt{L/C}$	$1.1\sqrt{2}\cdot\frac{m}{n}\cdot\sqrt{L/C}$	$1.1\sqrt{2}\cdot m\cdot\sqrt{L/C}$	$1.1\sqrt{2}\cdot\frac{m}{n}\cdot\sqrt{L/C}$
Output voltage	V_0	mV_0	mV_0	mV_0

FIG. 4.   The design of the hybrid mode LTD stage based on the Marx.

Figures 5 and 6 show the circuit model and calculation result of a hybrid mode LTD stage. Simulation results show that the stage's load output current amplitude and rise time are 1.025 MA and 105 ns (0–100%), respectively, and the load voltage is about 140 kV, under the conditions of capacitors charged to ± 40 kV, 0.14 Ω matched load and simultaneous switching.

IV. COMPONENT DEVELOPMENT

A. Long-life gas spark-gap switch

We demand the working parameters of the switch are ± 40 kV/20 kA, which is not too difficult for a gas spark-gap switch [16]. We also expect the switch to operate hundreds of thousands of shots, which is a key difficulty to overcome [17]. According to theoretical analysis, the factors affecting the lifetime of a gas spark-gap switch are mainly arc ablation of electrodes [18], contamination of the switch insulation shell because of electrode discharge products and the aging effect of the switch insulation shell under the action of a strong electric field [19]. In this paper, the main points of the switch design are: increasing the electrode discharge area to reduce local electrode ablation and controlling the flow direction of discharge products to reduce the pollution of the switch insulation structure.

The switch structure we developed is shown in Fig. 7. The switch adopts a three electrode configuration, where
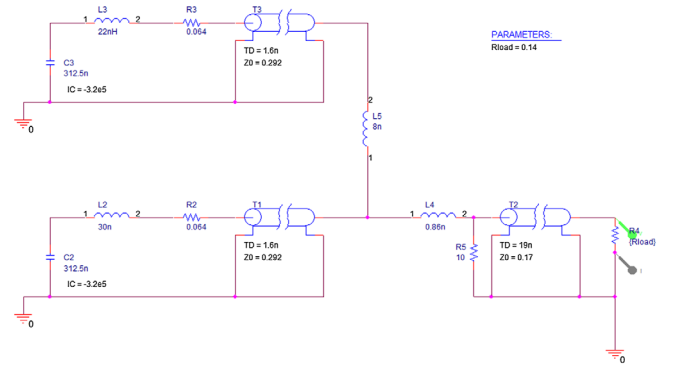

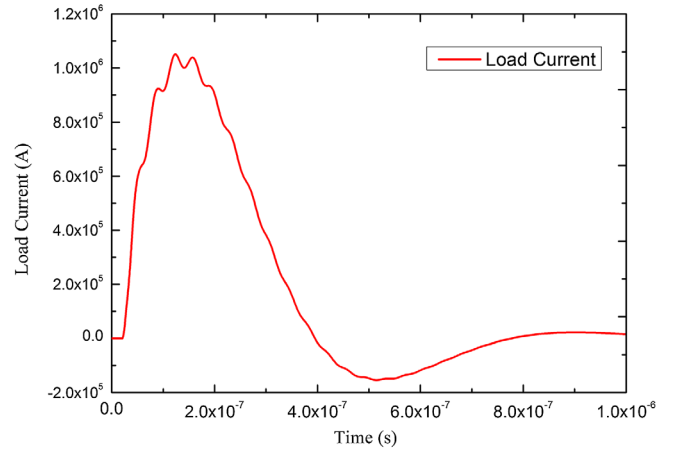FIG. 5.   The circuit model of a hybrid mode LTD stage.

FIG. 6.   Load current simulation result of a hybrid mode LTD stage.

the trigger electrode is coaxial with the main electrodes. The discharge area is located in the coaxial area between the main electrodes and the trigger electrode. The distribution of electric fields before and after the switch conduction time is shown in Fig. 8. The maximum electric field

TABLE II.   The relevant electrical parameters of each part.

| Part		Electrical parameters	Remarks
	Capacitor	Capacitance: 0.1 μF; Internal resistance: 0.2 Ω; Internal inductance: 35 nH	Work at ± 40 kV while design at ± 100 kV
Marx branch	Switch	Total inductance: 68 nH (structure inductance: 40 nH; spark channel inductance: 28 nH)	Structure inductance: $L_s = 200 \ln \frac{R_0}{R_i} \times h$ Spark channel inductance: $L_G = 14d$
	Coxial transmission line	Impedance: 6.9 Ω; Electrical length: 1.6 ns	Impedance: $R = \frac{60}{\sqrt{\varepsilon_r}} \ln \frac{R_0}{R_i}$ Electrical length: $\tau = l \times \sqrt{\varepsilon_r}/c$
	Transition zone (top layer)	Inductance: ~ 8 nH	Structure inductance: $L_s = 200 \ln \frac{R_0}{R_i} \times h$
Converging cavity	Radial transmission line	Inductance: 0.86 nH	Structure inductance: $L = \int_{R_i}^{R_0} \frac{\mu_0 h}{2\pi} dr = \frac{\mu_0 h}{2\pi} \ln \frac{R_0}{R_i}$
	Load	Line impedance: 0.17 Ω; Electrical length: 19.0 ns	Line impedance: $R = \frac{60}{\sqrt{\varepsilon_r}} \ln \frac{R_0}{R_i}$ Electrical length: $\tau = l \times \sqrt{\varepsilon_r}/c$
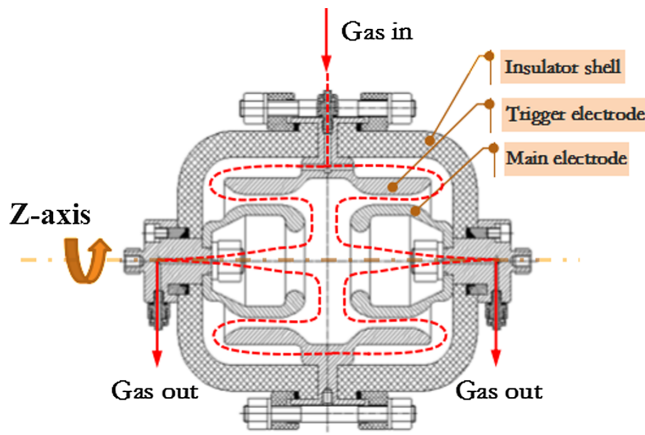
FIG. 7.   The configuration of long-life gas spark-gap switch.

area uniformly distributes in this area under the conditions of both charging and triggering. This configuration can greatly increase the effective electrode discharge area and improve the lifetime of the switch when the electrode ablation amount is certain. The gas inlet of the switch is located in the middle of the trigger electrode, and the outlets are located in the two ends of the main electrodes [20]. The insulation shell and electrode system constitute a special airflow path (as shown by the arrows in the figure), which keeps the discharge products completely separated
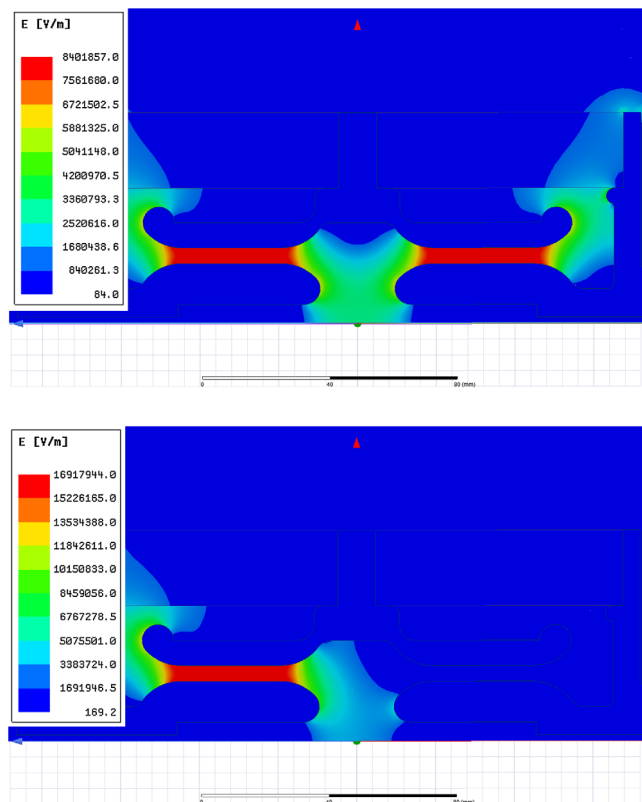
from the insulation shell, and effectively avoids deposition of the discharge products on the switch insulator. This design is expected to greatly improve the lifetime of the switch.

The designed and fabricated switch is placed in an experiment platform, which consists of the gas switch, trigger system, charging system, airflow control system and related auxiliary diagnosis system.

The lifetime assessment of the switch was carried out for the repeated frequency working conditions [± 40 kV/20 kA/0.1 Hz, gas pressure 0.4 MPa with pure N_2, at the highest flow rates of 15 Nm^3/h, "N" (nominal condition) means "standard temperature and pressure" (STP)]. The forced gas flow ensures removal of the arc residue and eroded electrode material from the switch. As a result, conducting material deposition is prevented and the surface of insulators is protected. The insulation resistance and the self-breakdown voltage of the switch were measured after each set of 1000 discharge shots. Results show that, although the breakdown voltage of the switch decreases slowly as the number of discharge shots increases, it basically remains stable after 50,000 shots. At present, the switch has been tested with over 172 000 shots, with no significant decline in performance. After multiple optimization steps (electrode configuration and insulation structure), the switch main electrode ablation result is shown in Fig. 9. It can be seen that the ablation situation is good. Since the effective discharge area of the electrode is rather large, relative uniform distribution of discharge spots is likely to lead to long lifetime of the switch, which is in line with the expected results.

B. Long-life capacitor

Because the load power in the LTD device comes directly from the capacitor discharge, there is no intermediate pulse compression process, so the performance requirements for the capacitor are very high [21]. In combination with the requirements of future energy devices, the main performance requirements of a capacitor are focused on the following aspects: high power level,

FIG. 8.   Electric fields distribution of charging and triggering time.

FIG. 9.   Electrode ablation result.

repetitive operation, long-life and high reliability [22]. High power level has two requirements for capacitors. First, capacitors are required to have high energy storage density. Second, capacitors are required to have low inductance, to achieve high current and short discharge time. The repetitive operation requires the capacitors to have low resistance to reduce heat loss, have good heat dissipation ability and temperature adaptability. Long life and high reliability require that capacitors have low partial discharge, low dielectric loss and high stability [23]. Considering that operating power and life are competing parameters, based on new energy storage materials, insulating materials and processes, we have optimized the internal electric field design and packaging process of the capacitor, balancing the power and lifetime parameters for the application of the electrical parameter range to develop high energy storage density and high reliability long-life pulse capacitor suitable for a fast pulse LTD.

A variety of capacitor energy storage materials and insulation media (such as polypropylene, polyester, polyimide, benzyl toluene, castor oil, linear alkyl benzene, etc.), as well as different types of electrode processes [24] (protruding foil type, non-salient polar type) were compared and analyzed, to clarify the relation between the process type and insulation materials. The design and technological approach of two typical high voltage pulse capacitors are preliminarily defined. One kind is based on polypropylene material, benzyl toluene insulation medium and protruding foil type. The other is based on polypropylene material, castor oil insulation medium, nonsalient polar type.

In comparison, the high voltage pulse capacitor based on polypropylene material, benzyl toluene insulation medium and protruding foil type has an obvious advantage in impedance, as shown in Table III, so we adopted this option and the structure and process were optimized.

We adopted the copper foil embedded cryogenic alloy welding process, which can reduce the connection resistance of the energy storage element in the capacitor provided that the end of the capacitor is not stretched. Also, the vortex-contact type process is applied on the outer electrode connection of the capacitor, which results in low resistance and high current of the high pulse voltage pulse capacitor and reduces the connection inductance. The size of the optimized high voltage pulse capacitor is reduced to $(110 \times 119 \times 119)$ mm^3, which further improves the energy storage density and greatly reduces the resistance and inductance. The experimental results showed that the internal resistance of the capacitor was reduced from 0.042 to 0.035 Ω by adopting the new electrode connection process, and the corresponding internal inductance was reduced from 45 to 25 nH.

During the life testing of the capacitor, some phenomena such as breakdowns, welding seam cracking and sealing failure were found. To address these technical problems, electric field shielding technology of the capacitor is proposed. This solves the problem of cumulative insulation aging of the capacitor end in the process of discharge voltage multiplication. Also, the sealing process of the integrated shell and the corner welding seam is reformed, so the insulation performance of the high voltage pulse capacitor is guaranteed.

To summarize, the improved electrode structure makes the electric field in the capacitor more uniform, the integral shell structure improves the sealing performance of the capacitor, and the copper foil embedded cryogenic alloy welding process can increase the flow capacity of capacitor discharge. Above all, the performance of capacitors with many innovative structures and processes has been greatly improved. The main performance parameters of the final capacitor are shown in Table IV.

TABLE III. Comparison of parameters of the high voltage pulse capacitors with two optimal designs.

Route	Dimensions/mm	Voltage/kV	Current/kA	Capacitance/nF	Impedance/Ω	Inductance/nH	Loss
Polypropylene material, Benzyl toluene insulation Medium, protruding foil type	$140 \times 140 \times 160$	50	25	100	≤ 0.043	≤ 45	$\leq 0.03\%$
Polypropylene material, Castor oil insulation medium, Nonsalient polar type	$140 \times 140 \times 160$	50	25	100	≤ 0.18	≤ 43	$\leq 0.04\%$

TABLE IV. Parameters of repetitive operation and the long-life high voltage pulse capacitor.

Parameter	Rated voltage	Operating current	Capacitance	Internal resistance	Internal inductance	Lifetime	Loss
Value	dc 50 kV	25 kA	100 nF	$\leq 0.035\ \Omega$	≤ 25 nH	$> 170\,000$	$\leq 0.03\%$

FIG. 10.   The system block diagram of four-stage coaxial Marx.

FIG. 12.   50 consecutive discharge waveforms of the four-stage Marx.
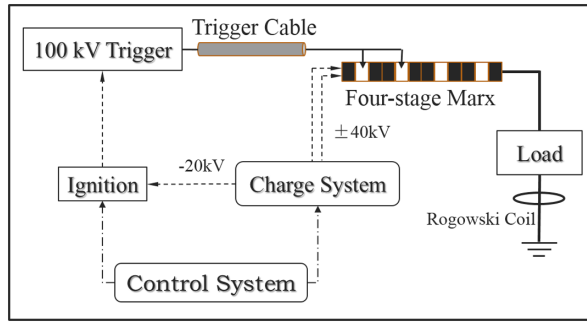
C. Four-stage coaxial Marx

A four-stage coaxial Marx is a component of the hybrid mode LTD stage. Its high voltage safety, Marx time jitter and output pulse front will all affect the whole stage's eventual performance [25]. So, it is necessary to verify the design of four-stage coaxial Marx based on gas switches to verify its design. The overall structure of the four-stage coaxial Marx and its insulation support and various interior connections were designed and optimized based on switch and capacitor prototypes of four-stage Marx experimental results, insulation design principles and electrical properties. The four-stage Marx system block diagram is shown in Fig. 10, and the final designed and processed coaxial Marx prototype is shown in Fig. 11.

The inductance and internal resistance parameters of the Marx branch are ascertained by the oscillation period and damping time to 1/e of the peak value of the experimental short-circuit discharge current waveform. The period of the discharge waveform is T = 607 ns. The capacitance of eight capacitors (each capacitance is 100 nF) in series is C_m = 12.5 nF. The inductance estimation from $L_m = T^2/4\pi^2 C_m \approx 747$ nH. The damping time to 1/e of the peak value is $T_{1/e} = 5.336$ μs, and the internal resistance estimation is $R_s = 2L_m/T_{1/e} \approx 0.28$ Ω.
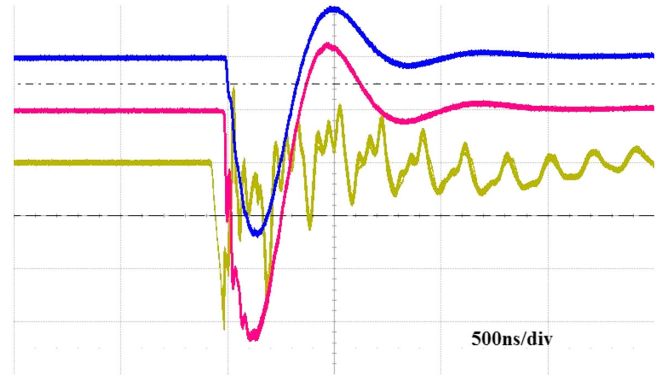

FIG. 11.   Picture of the four-stage coaxial Marx.

Figure 12 shows waveforms for 50 consecutive discharges of the four-stage Marx. Yellow lines represent the triggering waveforms, purple and blue lines represent the voltage and current waveforms, respectively. The four-stage Marx circuit's load current is about 21 kA, with a rise time of ∼90 ns (10%–90%), under the conditions of capacitors charged to ±40 kV and a 6.9 Ω matched load. The 50 consecutive discharge waveforms' delay time jitter is less than 4 ns (standard deviation), which shows good consistency.

In order to evaluate the performance of the four-stage coaxial Marx's repetitive and long-time continuous operation, relevant experiments were carried out. The experimental conditions were as follows: switches pressurized to 0.12 MPa with a gas mixture of nitrogen and sulfur hexafluoride (N_2 and SF_6); capacitors charged to ±40 kV; trigger voltage −50 kV; matched impedance condition; and the operation frequency was 0.1 Hz. The gas mixture of nitrogen and sulfur hexafluoride is used to isolate separate Marxes from their grounded envelopes.

The total number of shots was 20 183, over a 70 hour period including time for adjustments and diagnostic signal recording and analysis. The four-stage coaxial Marx worked stably during this testing period, and the output parameters did not change appreciably during more than 20 000 shots.

D. Repetitive multipath trigger system

A repetitive multipath trigger system is adopted for enabling a direct capacitor discharge technology system [26]. The components of the trigger system are shown in Fig. 13. The trigger system is composed of a former-trigger unit and a latter-trigger unit. When the former-trigger unit outputs five pulses, five switches of the corresponding latter-trigger unit are triggered. The latter-trigger unit outputs 50 pulses, and triggers 50 Marx branches of a hybrid mode LTD stage.

The former-trigger unit operates by direct discharge of capacitors through a switch [27]. In order to obtain fast
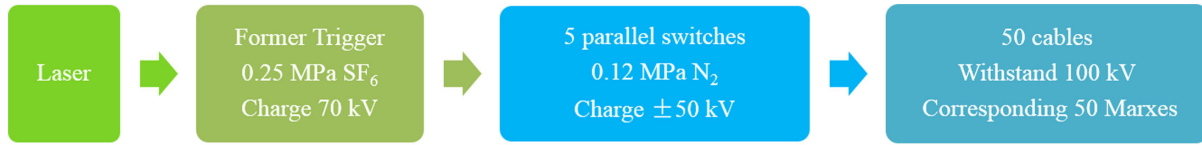
FIG. 13.   Diagram of the repetitive multipath trigger system.

pulse rise time, a minimized inductance design was used [28]. The overall structure is coaxial as shown in Fig. 14. Twenty 820 pF/120 kV ceramic capacitors are uniformly distributed around the circumference. The metal shell of the return conductor is as close as possible to ensure sufficient space for insulation, and the inductance of the coaxial structure is then small enough. The switch has a planar electrode configuration with small inductance. The output cable structure is matched in impedance to eliminate reflections.

The experimental results of the former-trigger unit show that when the charge voltage is 70 kV, an output pulse of about 70 kV is obtained on a matched load, and the pulse rise time is less than 20 ns (10%–90%). The configuration of the latter-trigger unit is shown in Fig. 15. The latter-trigger unit also adopts a direct capacitor discharge circuit, the output end is connected with the output cables, and the output cables are close to the cavity wall, so as to reduce the circuit inductance as much as possible. The latter-trigger unit consists of five groups in parallel, each with two 20 nF/120 kV main capacitors and a multigap switch in series. Each main capacitor is connected in parallel with two 1.5 nF/100 kV ceramic capacitors as harmonic capacitors. The harmonic superposition technique is used in the trigger system, so the proper pulse width and fast front are taken into account on the basis of the simple circuit of direct capacitor discharge.

The practical picture of the whole trigger system including former-trigger and latter-trigger units is shown in Fig. 16, and experimental output waveforms (ten consecutive shots) are shown in Fig. 17. Former-trigger unit outputs are ~70 kV (blue lines) when capacitors are charged to 70 kV. Latter-trigger unit outputs are ~50 kV (yellow, purple and green lines represent output voltages of three of the 50 cables), the rise times are less than 50 ns (10%–90%), pulse widths are more than 100 ns under the conditions of capacitors charged to ± 50 kV and five 7.5 Ω matched loads.

E. Reset system

The hybrid mode LTD stage does not have a Blumlein formation line structure. Therefore, only an external reset
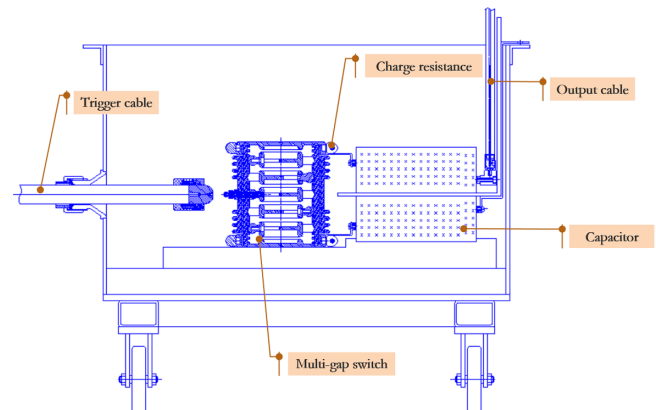

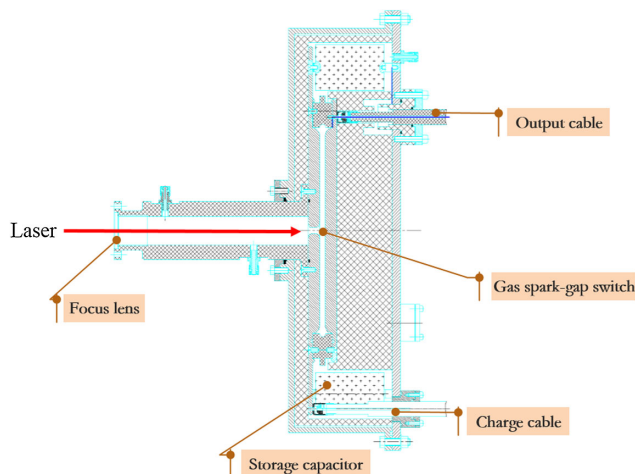FIG. 15.   Configuration of the latter-trigger unit.

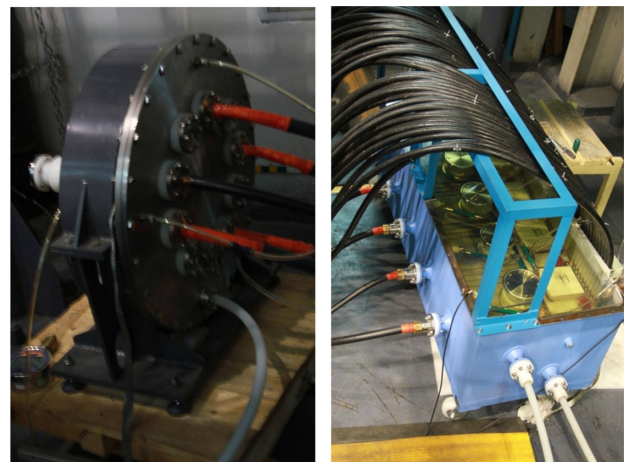FIG. 14.   Configuration of the former-trigger unit.

FIG. 16.   Practical pictures of the whole trigger system (left: former-trigger unit; right: latter-trigger unit).
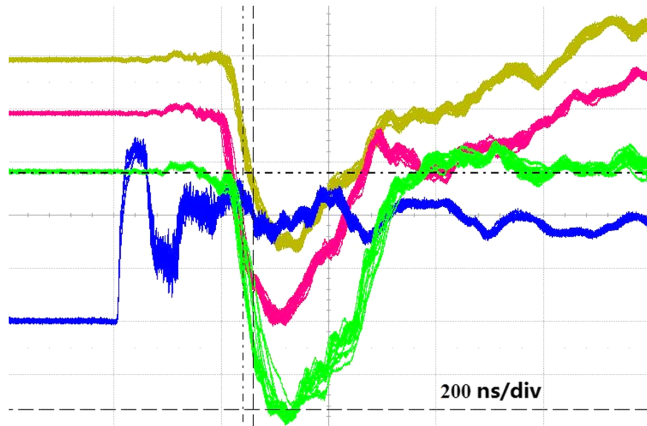
FIG. 17. Experimental output waveforms of the trigger system (ten consecutive shots).

system can be used for restoration [29,30]. The magnetic core in the reset circuit is in parallel with the load of the LTD stage, so the load must have a shunt effect on the reset current which will affect the normal operation of the reset system if a pulse current reset system is adopted. Meanwhile, the repetition rate of the hybrid mode LTD stage is about 0.1 Hz, and the experimental interval is only about 10 s. It is impossible to shut down the load in the main pulse discharge process. Taken into overall consideration, the reset process of the hybrid mode LTD stage is reset by a dc power supply, and the reset circuit topology and schematic diagram of the stage is shown in Fig. 18. Although the circuit inductance is large, because the influence of the inductance on the dc signal is very small, therefore, even if the solid resistance load is not switched off with the stage during reset process, the reset current shunt is still very small, and can be neglected.

The amorphous magnetic core's coercive force is about 8 A/m when tested at 50 Hz, the outer radius of the core is 77 cm, and the required dc reset current is 77.5 A. So, we use a dc power supply with maximum output of 200 V/80 A to reset the magnetic core. Because the pulse high voltage in the reset circuit is exactly the same as the main circuit voltage when the stage is discharged, the effective isolation of the high voltage pulse is a problem
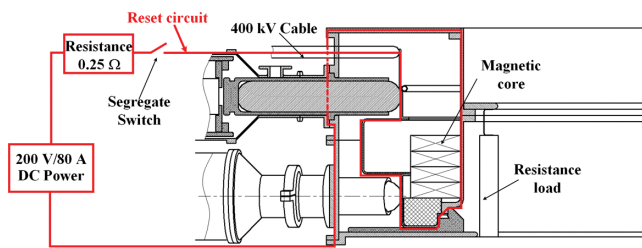
that must be considered. An isolation device is used to protect the reset circuit, and a solenoid valve is used to control the cylinder to drive the isolation switch. When the hybrid mode LTD stage is discharged, the switch is disconnected, and the switch is closed after the shot to reset the core. Both the solenoid valve and the dc power supply can be operated repetitively by remote control.

V. EXPERIMENTAL RESULTS OF HYBRID MODE LTD STAGE

After the feasibility of the technical approach and the above key technologies had been preliminarily verified, we completed the stage design, processing and installation. The corresponding hybrid mode LTD stage debugging experiment was carried out after the auxiliary systems were all in position. The installed stage is shown in Fig. 19.

During the debugging process, we encountered some problems such as the grounding capacitor of the Marx's first stage can breakdown in stage discharge, the insulation of the intersection of the transmission line and converging cavity is weak, and the synchronization of Marxes discharge times is not good enough. After solving these problems, the stage can run normally. However, when the capacitors are charged to ±40 kV, the load output voltage is only 125 kV (black line in Fig. 20), lower than the simulation result by ~10.7%. We suspect that core loss caused by insulation breakdown between amorphous magnetic core layers is occurring, which needs further verification. The next step is to change the amorphous magnetic core insulation process, with metallic glass ribbons insulated by insulation film such as Mylar instead of the SiO_2 layer produced by coating technology.

The whole stage's load output voltage is about 141.6 kV (red line in Fig. 20), with a rise time of ~112 ns (10%–90%); when the capacitors are charged to ±45 kV and the matched load is 0.14 Ω, the corresponding load current is ~1 MA. In addition, we have carried out a repetitive operation experiment, running more than 500 shots with ±40 kV charge, and the shortest time between shots is 12 s.

FIG. 18. Reset circuit topology and schematic diagram of the stage.

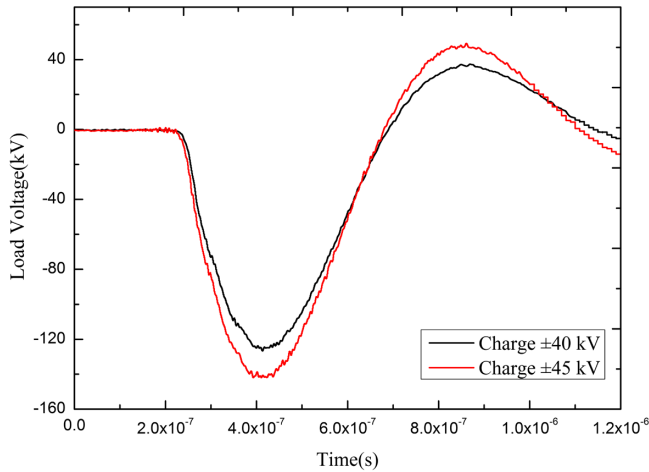FIG. 19. The installed hybrid mode LTD stage.

FIG. 20. Load output voltage waveforms of the hybrid mode LTD stage.

VI. SUMMARY

The technical feasibility of the hybrid mode LTD stage is preliminarily verified by the research reported in this paper, which shows that the design goal can be achieved through technical optimization. The LTD approach with compact coaxial Marxes replacing lower voltage bricks allows low component operating voltage and direct output fast pulse performance. The simpler trigger requirement of the Marx greatly reduces the requirement for the trigger system. The engineering complexity of the whole stage is also reduced. The hybrid mode LTD stage adopts a new circuit topology between pure series Marx and pure parallel LTD, expands the connotation of LTD technology, takes advantages of the two approaches and avoids their technical difficulties to a certain extent. At present, a hybrid mode LTD stage has been built, and the related technical objects have been basically achieved. However, the basic components, discharge circuit (Marx generator) and stage have potential for further optimization. The lifetime potential of the single stage needs to be evaluated with a large number of experiments, and the feasibility of the converging cavity and magnetic core also need further experimental verifications.

[1] M. K. Matzen, Pulsed power sciences at Sandia National Laboratories—The next generation, in *Proceedings of the 16th IEEE International Pulsed Power Conference, Albuquerque, NM* (IEEE, Piscataway, NJ, 2007), Vol. 1, pp. 1–15.

[2] C. L. Olson, Z-pinch inertial fusion energy, *Landholt-Boernstein Handbook on Energy Technologies* (2004), Vol. 8, p. 3, https://www.econologie.com/file/technologie_energie/Z-pinch.pdf.

[3] C. Deeney, P. D. LePell, T. Nash, B. Failor, S. L. Wong, R. R. Prasad, and M. C. Coulter, A review of Z-pinch research at Physics International, in *The 1992 9th International Conference on High-Power Particle Beams* (IEEE, Washington, 1992), Vol. 1, pp. 159–166, http://ieeexplore.ieee.org/abstract/document/6306485/.

[4] R. B. Spielman, F. Long, T. H. Martin, J. W. Poukey, D. B. Seidel, W. Shoup, W. A. Stygar, D. H. McDaniel, M. A. Mostrom, K. W. Struve, P. Corcoran, I. Smith, and P. Spence, PBFA II-Z: A 20-MA driver for Z-pinch experiments, in *The Tenth IEEE International Pulsed Power Conference, 1995, Digest of Technical Papers* (IEEE, Albuquerque, 1995), Vol. 1, pp. 396–404, http://ieeexplore.ieee.org/abstract/document/596512/.

[5] A. N. Bastrikov, A. A. Kim, B. M. Kovalchuk, E. V. Kumpjak, S. V. Loginov, V. I. Manylov, and L. Frescaline, Fast primary energy storage based on linear transformer scheme, in *The 11th IEEE International Pulsed Power Conference, 1997, Digest of Technical Papers* (IEEE, Baltimore, 1997), Vol. 1, pp. 489–497.

[6] A. A. Kim, B. M. Kovalchuk, A. N. Bastrikov, V. G. Durakov, S. N. Volkov, and V. A. Sinebryukhov, 100 ns current rise time LTD stage, in *Pulsed Power Plasma Science, 2001, PPPS-2001, Digest of Technical Papers* (IEEE, Las Vegas, 2001), Vol. 2, pp. 1491–1494, http://ieeexplore.ieee.org/abstract/document/1001840/.

[7] L. Zhou, J. Deng, L. Chen, W. Zou, M. Wang, W. Xie, and L. Yang, Status of linear transformer driver research, High Power Laser Part. Beams **20,** 1947 (2008).

[8] L. Chen, L. Zhou, W. Xie, S. Feng, J. Ren, S. Wu, and W. Qin, Research on 100 kA fast linear transformer driver stage, J. High Power Laser Part. Beams **6,** 056 (2010).

[9] M. Wang, L. Zhou, W. Zou, W. Xie, Z. Yang, and L. Chen, Mixed-mode LTD module, High Power Laser Part. Beams **24,** 1239 (2012).

[10] X. S. Liu, *High Power Pulsed Technology* (National Defense Industry Press, Beijing, 2005).

[11] K. T. Lancaster, R. S. Clark, and M. T. Buttram, A compact, repetitive, 6.5 kilojoule Marx generator, in *IEEE Conference Record of the 1988 Eighteenth Power Modulator Symposium* (IEEE, Hilton Head, 1988), pp. 48–51, http://ieeexplore.ieee.org/abstract/document/26234/.

[12] M. M. Kekez, High repetition rate compact Marx generator, in *The 14th IEEE International Pulsed Power Conference, 2003, Digest of Technical Papers. PPC-2003* (IEEE, Dallas, 2003), Vol. 2, pp. 1427–1430, http://ieeexplore.ieee.org/abstract/document/1278084/.

[13] A. A. Kim, A. N. Bastrikov, S. N. Volkov, V. G. Durakov, B. M. Kovalchuk, and V. A. Sinebryukhov, 100 GW fast LTD stage, in *Proceedings of the 13th International Symposium High Current Electron* (2004), pp. 141–144, http://www.congress-2006.hcei.tsc.ru/cat/proc_2004/13/Paper_034.pdf.

[14] X. Peng and Z. Wang, Conceptual research on Z-pinch driven fusion-fission hybrid reactor, High Power Laser Part. Beams **26,** 090201 (2014).

[15] J. Deng, J. Shi, W. Xie, L. Zhang, S. Feng, J. Li, and Q. Li, Overview of pulsed power research at CAEP, IEEE Trans. Plasma Sci. **43,** 2760 (2015).

[16] L. Zhang, M. Wang, W. Han, J. Jiang, J. Ren, J. Kang, and L. Zhou, Design and experiment of long lifetime coaxial-electrode gas spark switch, High Power Laser Part. Beams **28,** 015024 (2016).

[17] G. Schaefer, M. Kristiansen, and A. Guenther, *Gas Discharge Closing Switches* (Plenum Press, New York, 1990).

[18] M. He, C. He, and J. Li, Research on erosion of gas spark switch electrodes, High Voltage Eng. **10,** 022 (2004).

[19] S. J. MacGregor, S. M. Turnbull, F. A. Tuema, and O. Farish, Factors affecting and methods of improving the pulse repetition frequency of pulse-charged and dc-charged high-pressure gas switches, IEEE Trans. Plasma Sci. **25,** 110 (1997).

[20] G. J. J. Winands, Z. Liu, A. J. M. Pemen, E. J. M. Van Heesch, and K. Yan, Long lifetime, triggered, spark-gap switch for repetitive pulsed power applications, Rev. Sci. Instrum. **76,** 085107 (2005).

[21] F. MacDougall, R. Jow, J. Ennis, S. P. S. Yen, X. C. Yang, and J. Ho, Pulsed power capacitors, in *Proceedings of the 2008 IEEE International Power Modulators and High Voltage Conference* (IEEE, Las Vegas, 2008), pp. 167–169, http://ieeexplore.ieee.org/abstract/document/4743606/.

[22] T. R. Jow, F. W. MacDougall, J. B. Ennis, X. H. Yang, M. A. Schneider, C. J. Scozzie, and S. P. S. Yen, Pulsed power capacitor development and outlook, in *The 2015 IEEE Pulsed Power Conference (PPC)* (IEEE, Austin, 2015), pp. 1–7, http://ieeexplore.ieee.org/abstract/document/7297027/.

[23] N. I. Boyko, A. N. Tur, V. V. Rudakov, L. S. Evdoshenko, A. I. Zarochentsev, and V. M. Ivanov, High-voltage pulse capacitors with a resource of 10(11) pulses, Instrum. Exp. Tech. **42,** 371 (1999).

[24] M. M. Kasumov and V. A. Chudakov, Modification of a pulse capacitor for operating at a high current of periodic discharge, Instrum. Exp. Tech. **38,** 121 (1995).

[25] S. K. Lam, R. Miller, L. Sanders, P. Sincerny, and T. Tucker, Fast Marx for PRS drivers, in *The 14th IEEE International Pulsed Power Conference, 2003, Digest of Technical Papers, PPC-2003* (IEEE, Dallas, 2003), Vol. 1, pp. 619–621, http://ieeexplore.ieee.org/abstract/document/1277786/.

[26] M. E. Savage and B. S. Stoltzfus, High reliability low jitter 80 kV pulse generator, Phys. Rev. ST Accel. Beams **12,** 080401 (2009).

[27] F. J. Zutavern, K. W. Reed, S. F. Glover, A. Mar, M. H. Ruebush, M. L. Horry, and T. L. Smith, Fiber-optic controlled PCSS triggers for high voltage pulsed power switches, in *The 2005 IEEE Pulsed Power Conference* (IEEE, Monterey, 2005), pp. 810–813, http://ieeexplore.ieee.org/abstract/document/4084341/.

[28] F. J. Zutavern, J. C. Armijo, S. M. Cameron, G. J. Denison, J. M. Lehr, T. S. Luk, and J. V. Rudd, Optically activated switches for low jitter pulsed power applications, in *The 14th IEEE International Pulsed Power Conference, 2003, Digest of Technical Papers, PPC-2003* (IEEE, Dallas, 2003), Vol. 1, pp. 591–594, http://ieeexplore.ieee.org/abstract/document/1277780/.

[29] D. M. Barrett, Core reset considerations in magnetic pulse compression networks, in *The Tenth IEEE International Pulsed Power Conference, 1995, Digest of Technical Papers* (IEEE, Albuquerque, 1995), Vol. 2, pp. 1160–1165, http://ieeexplore.ieee.org/abstract/document/599771/.

[30] R. Burdt, R. D. Curry, K. F. McDonald, P. Melcher, R. Ness, and C. Huang, Evaluation of nanocrystalline materials, amorphous metal alloys, and ferrites for magnetic pulse compression applications, J. Appl. Phys. **99,** 08D911 (2006).